Ultrasound in Med. & Biol., Vol. 28, No. 5, pp. 617–624, 2002

0301-5629/02/$–see front matter

PII: S0301-5629(02)00503-3

● *Original Contribution*

CORRELATION OF ULTRASOUND PHASE WITH PHYSICAL SKULL PROPERTIES

G. T. CLEMENT and KULLERVO HYNYNEN
Department of Radiology, Brigham & Women's Hospital, Harvard Medical School, Boston, MA, USA

(*Received* 21 *August* 2001; *in final form* 20 *February* 2002)

Abstract—Noninvasive treatment of brain disorders using focused ultrasound (US) requires a reliable model for predicting the distortion of the field due to the skull using physical parameters obtained *in vivo*. Previous studies indicate that control of US phase alone is sufficient for producing a focus through the skull using a phased US array. The present study concentrates on identifying methods to estimate phase distortion. This will be critical for the future clinical use of noninvasive brain therapy. Ten *ex vivo* human calvaria were examined. Each sample was imaged in water using computerized tomography (CT). The information was used to determine the inner and outer skull surfaces, thickness as a function of position, and internal structure. Phase measurement over a series of points was obtained by placing a skull fragment between a transducer and a receiver with the skull normal to the transducer. Correlation was found between the skull thickness and the US phase shift. A linear fit of the data follows that predicted by a homogeneous skull when average speed of sound 2650 m/s was used. Large variance (SD = 60°, mean = 50°) indicates the additional role of internal bone speed and density fluctuations. In an attempt to reduce the variance, the skull was first studied as a three-layer structure. Next, density-dependent bone speed fluctuation was introduced to both the single-layer and three-layer models. It was determined that adjustment of the mean propagation speeds using density improves the overall phase prediction. Results demonstrate that it is possible to use thickness and density information from CT images to predict the US phase distortion induced by the skull accurately enough for therapeutic aberration correction. In addition, the measurements provide coefficients for phase dependence on skull thickness and density that can be used in clinical treatments. (E-mail: clement@bwh.harvard.edu) © **2002 World Federation for Ultrasound in Medicine & Biology.**

Key Words: **Ultrasound, Skull.**

INTRODUCTION

Numerous studies have examined the effects of ultrasound (US) on the brain (Robinson and Lele 1972; Fry 1954; Fry et al. 1981) and its potential as a therapeutic and surgical tool. The prospect of performing noninvasive US procedures through the intact skull (Fry and Goss 1980; Hynynen and Jolesz 1998) makes focused US a particularly appealing treatment method. However, transcranial propagation of US severely distorts both amplitude and phase of the wave, causing defocusing of the beam. Previous studies have shown that a focus distorted by a human skull can be reconstructed by adjusting only the driving phase of US transducer elements (Smith et al. 1986; Hynynen and Jolesz 1998; Thomas and Fink 1996). This is particularly important when large-aperture arrays are used (Sun and Hynynen 1999; Clement et al. 2000a). To date, correction has been obtained by using hydrophone probes placed at the desired focal location within *ex vivo* skull samples. It has been proposed that this phase correction can be done completely noninvasively by using modern imaging methods (magnetic resonance imaging or MRI, computerized tomography or CT) to provide input for mathematical models (Sun and Hynynen 1998). The most accurate of these devices for providing information about the inner and outer surfaces of the skull bone is CT. The thickness of the skull is a major factor in US phase distortion because the speed of sound in bone (about 2700 m/s) is significantly higher than in water or soft tissues (about 1500 m/s). In addition, it is known from the work of Fry and Barger (1978) that the sound speed varies significantly across three discrete bone layers, the inner and outer cortical layers and a central tra-

Address correspondence to: G. T. Clement, M.D., Department of Radiology, Harvard Medical School, 221 Longwood Ave., #007, Boston, MA 02115 USA. E-mail: gclement@hms.harvard.edu

becular layer. These layers are clearly visible in CT images. The sound speed in bone is density-dependent. CT images can also provide bone density as a function of position.

In this study, we tested the feasibility of using CT-derived skull density and layer information to predict US phase distortion. We tested US propagation models by obtaining CT scans of *post mortem ex vivo* human skulls and compared these properties to the US phase after passing through the skull. This test is a critical first step toward the establishment of completely noninvasive focusing through the skull.

Specifically, four models were investigated that predict US phase after propagating through the skull. The initial model assumes the skull to be a homogeneous structure, with constant density and sound speed. Skull thickness is, thus, the sole variable controlling shifts in the US phase through different points on a skull surface. The second model divides the skull into three layers; the outer cortical layer, the central trabecular layer and the inner cortical layer. For each layer, a constant speed of sound, as measured by Fry and Barger (1978), was applied. The third and fourth models introduce a density-dependent speed variation into the single-layer and three-layer models, respectively. An effective sound speed that is a function of the density variation was applied to each layer.

Each of the abovementioned models assumes that the measured phase is constant in time. However, high-power therapeutic operation is expected to produce a momentary temperature rise in the skull between 5°C and 10°C, changing both the density (Wear 2000) and sound speed, potentially causing a significant shift in US phase. A set of measurements examines the phase difference between US propagated through bone at various temperatures. These measurements will provide the experimental data needed for the clinical implementation of noninvasive transcranial US treatments of the brain.

METHODS

Experimental procedure

A total of 10 *ex vivo* calvaria (brain cages) were used in the study. These skulls were fixed in formaldehyde, which has been shown to maintain the bone properties of a fresh skull (Fry and Barger 1978). To perform phase measurements, a calvarium was inserted between a single transducer and a needle hydrophone, as shown in Fig. 1. The transducer was a 0.51-MHz PZT disk cut in-house to 5×7 mm^2, mounted with an air backing. The frequency and dimensions are similar to that of a previously studied array designed for transskull therapy (Clement et al. 2000b). The hydrophone was a 0.2-mm

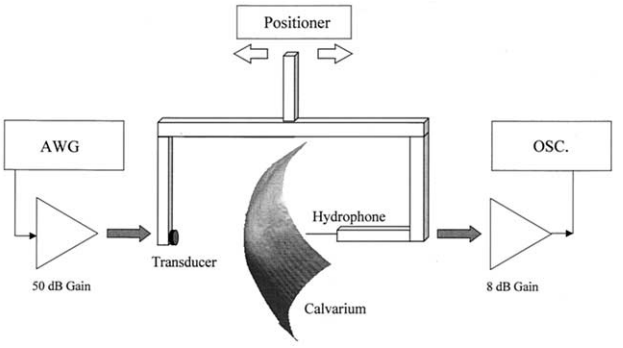

Fig. 1. The experimental setup for measuring phase shifts due to the skull.

PVDF membrane (Precision Acoustics, Dorchester, UK). The transducer and hydrophone were mounted at a constant distance of 14 cm from each other and the calvarium was placed approximately 3 cm from the transducer for measurement, so that the skull surface was approximately parallel with the transducer face. The transducer input was a 20-cycle 0.51-MHz sinusoid generated by an arbitrary waveform generator (Wavetek, model 305, Everett, WA) and fed to a power amplifier (ENI, model 3100L, Rochester, NY). Hydrophone response was sent through a Precision Acoustics preamplifier and recorded by a digital oscilloscope (Textronix, model 380, Beaverton, OR). To avoid interference from reflection off the hydrophone holder and tank walls, only the first 20 μs of the received time trace was considered.

For measurement location on a calvarium, the acoustic waveform was recorded 5 times. Before each subsequent measurement, the skull was removed and then reinserted between the transducer and hydrophone. Each trial was intended to direct US through the same location. The waveform resulting from direct propagation through the water without a skull was also recorded. For reference, the skull was permanently marked with ink at the point of each measurement. At each point, the skull thickness was measured using mechanical calipers. A total of 1000 waveforms were measured for 200 positions distributed over the skulls. The phase was determined relative to the driving signal and was calculated from the Fourier transform of the recorded waveform.

To examine the internal structure of the skulls, CT images of each calvarium were obtained. The skulls were imaged with a scanner (Siemens SOMATOM, Munich, Germany, using an AH50 kernel) along 1-mm slices digitized to a 512×512 matrix over a 200×200 mm^2 field of view. These bone images were manually divided into three regions determined by relative image intensity: they were the inner table, outer table and the central layer. A CT image showing the internal bone layers is presented in Fig. 2. Registration between the US mea-

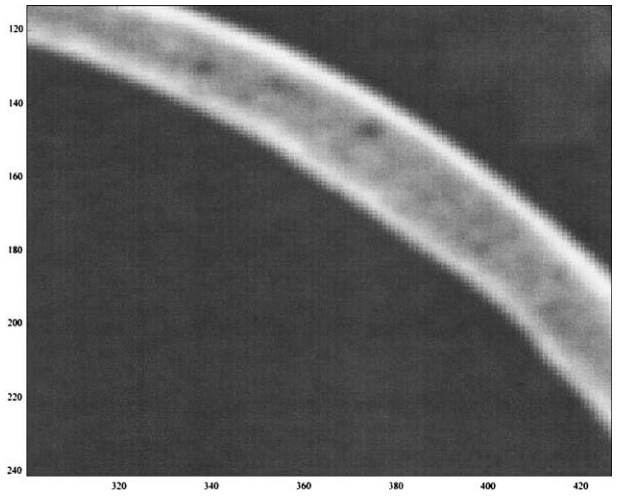

Fig. 2. CT section of a skull bone in water. The cortical inner and outer cortical layers are brighter (denser) and more homogeneous than the central trabecular layer.

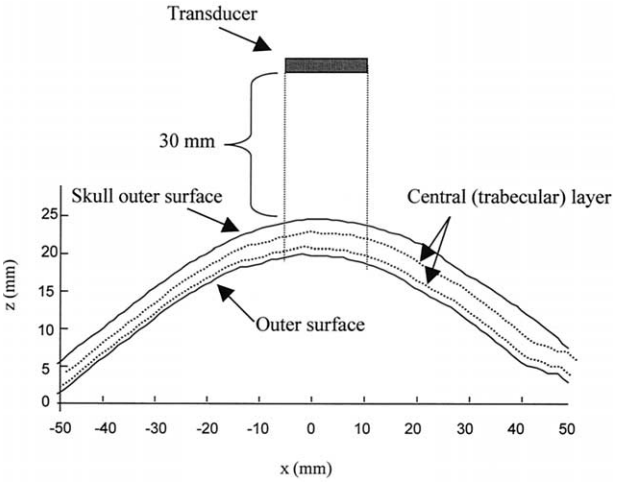

Fig. 3. Illustration of the transducer alignment relative the skull. The layers of the skull are treated as parallel plates. For each measurement position, the mean density directly below the transducer was determined from CT images.

surement locations and the CT thickness measurements was achieved by combining the CT images of a skull into a composite image and overlaying it with a digital photograph of the marked skull. The overlay was used to select the image slice and position of each measurement location. To verify the selected location on the CT image, caliper measurements were compared with the CT thickness measurements.

Single-layer approach

Near-normal propagation through homogeneous skull bone is assumed for the single-layer model, illustrated in Fig. 3. A simple relation expresses the phase shift due to propagation through a given point on the skull:

$$\phi = 2\pi f D\left(\frac{1}{c_0} - \frac{1}{c_s}\right), \tag{1}$$

where the frequency is $f = 5.1 \times 10^5$ Hz, the sound speed in water taken at room temperature is $c_0 = 1.49 \times 10^3$ m/s, the speed in the skull bone is $c_s = 2.65 \times 10^3$m/s, and D is the thickness of the skull, which is assumed constant over the US beamwidth. This convention of subtracting the phase shift due to direct propagation of the field in water from the shift due to the skull provides a positive phase shift.

Three-layer approach

The three-layer model assumes that the skull consists of three homogeneous layers, as shown in Fig. 3. The speed of sound is assumed to be 2.5×10^3 m/s for the central layer and 2.9×10^3 m/s for the inner and outer layers (Fry and Barger 1978). The expected phase shift across the skull is then determined as:

$$\phi = 2\pi f \sum_{n=1}^{3} D_n\left(\frac{1}{c_0} - \frac{1}{c_n}\right), \tag{2}$$

with c_n equal to the layer speed and D_n is the thickness of the nth layer.

Correction for density variation

To this point, both the single-layer and three-layer models have assumed that the sound speed is constant within a given bone layer. However, CT scans indicate that there is appreciable density variation within these layers, so any correlation between skull density and sound speed will contribute to the overall phase error. The density correction models attempt to reduce this error by replacing the sound speed c_s in eqn (1) and c_n in eqn (2) with an effective sound speed that is a function of the mean density across the sample c_{eff}. This speed is called "effective" because it does not represent the actual sound speed but, rather, it is given by:

$$c_{\text{eff}} = \left[\frac{1}{D}\int_0^D \frac{dr}{c(\rho(r))}\right]^{-1}, \tag{3}$$

where c and ρ represent the density and speed at position r. The CT reconstruction kernel assigns each 0.15 mm^2 $\times$ 1 mm slice thickness voxel an intensity value

equal to the density of the material. Mean density was determined by summing the CT intensity values along the axis of propagation inside the bone and dividing by the total number of summed voxels.

Using the measured phase shift, the effective sound speed for a layer was obtained by inverting eqn (1):

$$c_s = \left[\frac{1}{c_0} - \frac{\phi}{2\pi f D}\right]^{-1}. \quad (4)$$

Because ϕ provides only the principal value of the argument, the method selects the even integer multiple of the principal of the argument producing the speed closest to the Fry and Barger (1978) reported value of 2650 m/s. At a frequency of 0.51 MHz, and with a typical skull thickness of 12 mm, this would allow a speed range between 2180 m/s to 3390 m/s over a 2π phase interval. The effective speed would then be calculated as a function of density from a polynomial curve fit:

$$c_{\text{eff}}(\rho) = \sum_{n=0}^{N} A_n \rho^{N-n}, \quad (5)$$

with $N + 1$ coefficients A_n to be determined for an Nth degree fit.

To extend the method to three layers, the optimal effective sound speed for the individual layers was determined using a least squares method. The best fit sound speeds for 1. the inner and outer layers of the skull and 2. the inner matrix of the skull were acquired by a least squares fit of c_i:

$$\left\| \left[\frac{d_1 + d_2 + d_3}{c_0} - \frac{d_2}{c_{\text{ii}}} - \frac{\phi}{2\pi f}\right] c_i = d_1 + d_3 \right\|, \quad (6)$$

without *a priori* knowledge of c_{ii}, by minimizing the equation over the range from 1400 m/s to 4000 m/s.

To test the density correction methods, new data were obtained from a second sample consisting of 89 locations taken over 8 of the previously measured calvaria. Care was taken that the new locations did not coincide with the initial sample used to obtain the correction factor. Three measurements were made at each of these locations and the average value was used. Equipment and methodology were similar to that used in the first sample.

Model assessment

The goal of phase correction in transskull US therapy is to combine the fields from each element so that they are in phase with each other at the focal point. The quality of a given model may then be assessed by its ability to perform this phasing. For a transducer with N elements, the peak pressure amplitude at the focus will be reduced by an amount:

$$\frac{P}{P_0} = \left| \sum_{n=1}^{N} e^{i\phi_n} \right|, \quad (7)$$

due to the phase error ϕ_n introduced by incorrect prediction of the phase through the skull, assuming an ideal situation where the skull attenuation from each transducer element is identical. For example, if the model successfully corrects the phase shift (zero phase error) in each of the N cases, the final pressure amplitude will be $P = N \times P_0$.

To assess the quality of each model, a phase error probability distribution was formed from the previous phase measurements through the 10 skulls. The distribution consisted of the percent of the total measured points as a function of the magnitude of the phase error between the model and measurements. To simulate a model's expected amplitude loss for an N-element array, a pseudorandom data set was generated. First, a candidate value lying between $-\pi/2$ and $\pi/2$ radians with equal probability was obtained. The likelihood that the candidate would become a member of the data set was then determined from the phase error probability distribution. When a predetermined number of phase errors ($n = 1000$) had been chosen, the acoustic pressure amplitude at the focus was calculated by eqn (7). A practical array for brain therapy is expected to contain on the order of 1000 elements (Sun and Hynynen 1999).

Thermal effects

High-intensity therapy through the skull is expected to cause a measurable rise in skull temperature. In turn, thermal fluctuation of the bone will cause changes in both density and sound speed, which are not considered in the above models. To determine if these changes significantly affect the US phase, an experiment was performed to measure temperature-dependent phase shifts. The experimental setup and procedure were identical to that described above, except that the skull was heated to a known temperature before placing it into the measurement tank, and a 0.665-MHz transducer was used. The skull was heated by placing it in a circulated temperature-controlled water bath, allowing sufficient time for the skull to reach water temperature. For measurement, the skull was rapidly removed from the bath and placed in the measurement tank. Waveforms were recorded imme-

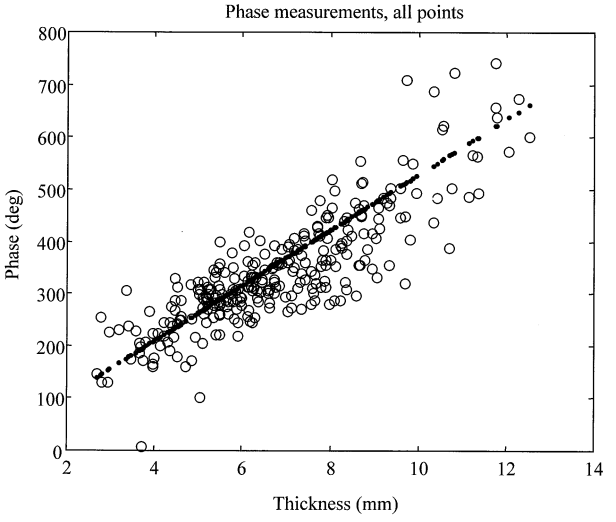

Fig. 4. Phase shift caused by skull at 0.51 MHz as a function of skull thickness.

diately to minimize heat transfer between the skull and the water bath because both heating of the water and cooling of the skull could potentially alter the measurements. The skull and water were allowed to cool to a base temperature of 22°C and the waveform through the skull was again recorded, allowing the change in phase due to bone heating to be calculated. Waveform data were obtained for skull temperatures at 50°C, 40°C, 30°C and 22°C.

RESULTS

The phase shift through a single layer calculated using eqn (1) is plotted along with all measured phase shifts in Fig. 4. The SD of the equation over 200 separate skull locations is calculated to be 60° with a mean value of 50°. Additional information is revealed in Fig. 5, showing the percent of points differing by more than a given phase angle ϕ from the calculated value. For example, an even distribution of phase error between 0° and 180° would produce a straight line extending from 100% at 0° to 0% at 180°, as illustrated by the straight line across the figure. A sharp decay then indicates good correlation between the experiment and the model. The measurements plotted in terms of this difference reveal that half of all measured points deviate by 45° or more, but only 15% deviate by more than 90°. A linear least squares fit of the data presented in Fig. 4 was performed to find the sound speeds that minimize the SD. A sound speed of 2.77×10^3 m/s was obtained. Using this sound value in eqn (1), the SD was reduced only to 59°, as opposed to an SD of 60° obtained using the Fry and Barger (1978) tabulated value of 2.65×10^3 m/s.

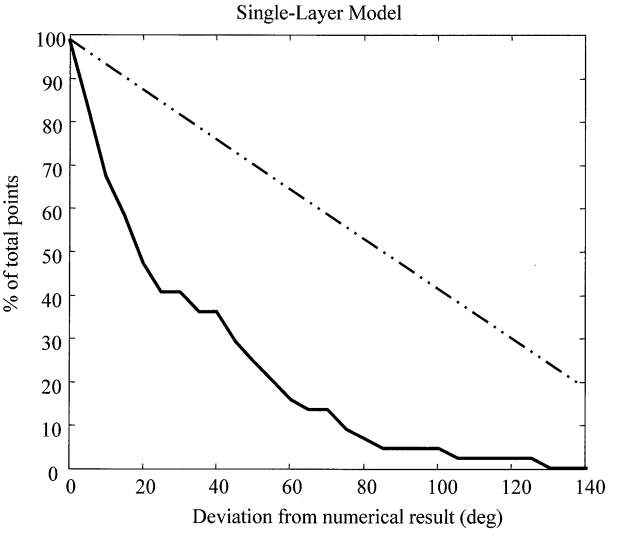

Fig. 5. Magnitude of error in single-layer skull model with a fixed sound speed of 2650 m/s as a percentage of total points (—). (– · · –) = the distribution expected if there is zero correlation between the model and measurements.

The second model, which assumes three bone layers, was calculated using eqn (2). Deviation of the measured points from their expected values as a percentage of the total number of points is shown as the solid line in Fig. 6. Introduction of these additional layers was found to produce only a small change in the deviation between the measured and expected values, compared with the single-layer result obtained using a

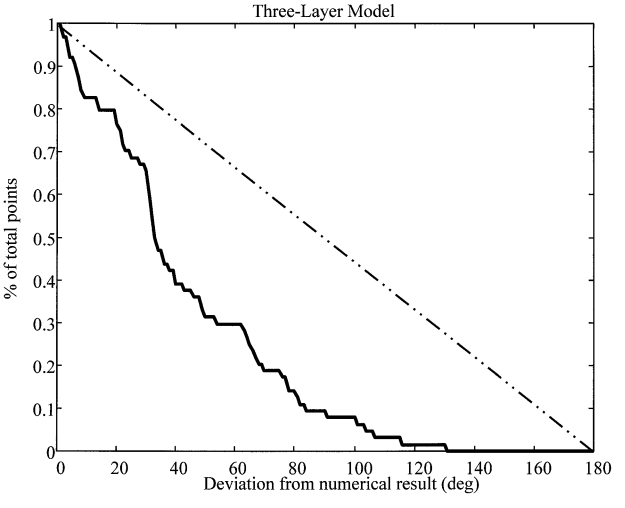

Fig. 6. Magnitude of error in three-layer skull model using tabulated data-fit sound speeds of 2450 m/s for trabecular bone and 3150 m/s for cortical bone as a percentage of total points (—). (– · · –) = the distribution expected if there is zero correlation between the model and measurements.

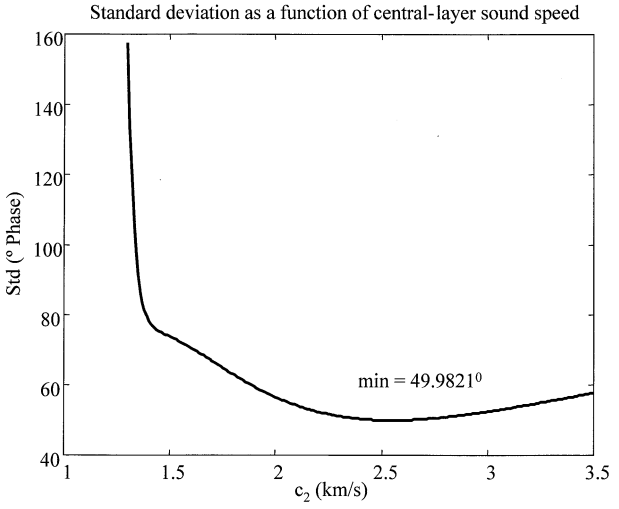

Fig. 7. Curve showing minimization of the three-layer bone model when a trabecular sound speed of 2450 m/s was used. The cortical speed was held constant at 3150 m/s.

constant sound speed of 2.65×10^3 m/s. Similar to the single-layer case, a least squares fit was performed to find the sound speeds that minimize the SD. The relation between c_i and c_{ii} is shown in Fig. 7, where the optimal values were selected by finding the minimum SD over the surface. An effective sound speed of 2.45×10^3 m/s was found for the central layer and 3.15×10^3 m/s for the outer layers. However, when these sound speeds were applied to the three-layer model, no significant improvement in the overall correlation with the measured data were observed.

The third model, which applies an empirical density correction to the single-layer model, improves the overall correlation with the measured data. A first-order (linear) fit obtained using eqn (5) yields the equation:

$$c_{\text{eff}} = 2.06 \frac{m^4}{\text{s kg}} \rho - 1.54 \times 10^3 \frac{m}{s} \tag{8}$$

in MKS units over the range of thickness-averaged densities between 1.82×10^3 kg/m^3 and 2.45×10^3 kg/m^3 and at the operating frequency of 0.51 MHz. Results are displayed in Fig. 8, showing 50% of all points to deviate by less than 38°, as opposed to 45° in the single-layer model without correction. Similarly, a fourth order fit of the data yields the following expansion coefficients for eqn (5):

$A_0 = 2.558e - 005$ $A_1 = -0.2276$
$A_2 = 752.9$ $A_3 = -1.09e + 006$
$A_4 = 5.94e + 008.$

The density correction was also applied to the three-layer model, obtaining separate data for cortical and trabecular bone. For the layers, linear fits of:

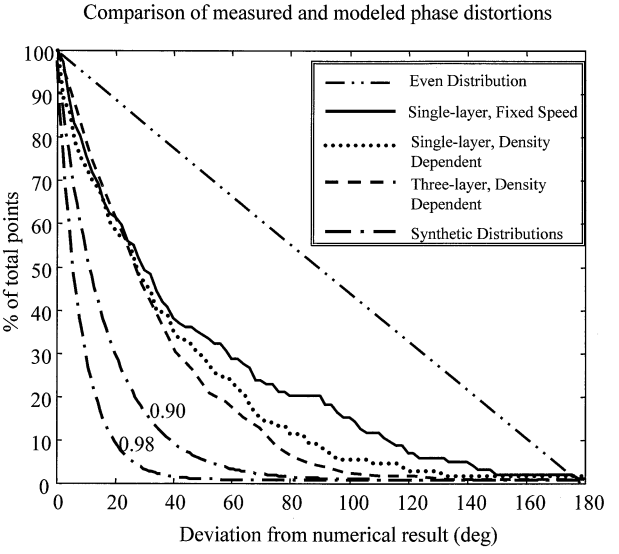

Fig. 8. Comparison of the single-layer homogeneous bone model (—) with a single-layer density-variant model (· · ·) and a three-layer density-variant model (- - -). Additional curves (–·–·–) show distributions required to achieve 90% and 98% of the peak pressure, when all sources arrive in phase.

$$c_c = 2.11 \frac{m^4}{\text{s kg}} \rho - 1300 \frac{m}{s} \tag{9}$$

$$c_t = 1.84 \frac{m^4}{\text{s kg}} \rho - 840 \frac{m}{s} \tag{10}$$

were determined and are displayed as the dashed line in Fig. 8.

Change in peak acoustic pressure through the skull due to the introduction of error into the phase was investigated using the synthetic data in the Methods section. If multiple transducer elements are used to produce a focused US field, the focus will occur at the point where all elements are in phase. A 1000-element point source "transducer" was considered. First, a probability distribution was generated by normalizing the single-layer distribution function presented in Fig. 5. All elements were given the same amplitude, but the elements have a phase error distribution similar to the figure. The pressure field was calculated to be 63% of the ideal phase-corrected value, when all sources arrive in phase. Next, the algorithm was run with a phase error introduced according to the distribution from the single-layer model with density correction. Addition of this empirical correction (Fig. 7, dotted) improves the peak pressure amplitude to 76% of the ideal value. The three-layer density variant model was tested with the sound speed fits, given by eqn (9), that present the best overall agreement with the measured data. The error distribution

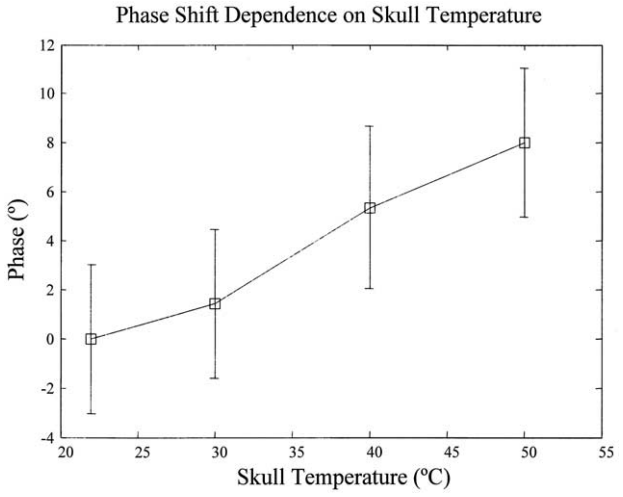

Fig. 9. Change in phase through the skull as a function of temperature at 0.665 MHz.

displayed as a dashed curve in Fig. 8 predicts a pressure amplitude of 79% of the ideal value. The error distributions from these results were also compared with two synthetic cases. These are the normalized error distributions required to achieve 90% and 98% of the peak pressure expected when all sources arrive in phase.

All of the above results were performed at room temperature. Measurements at temperatures near body temperature (37°C), and at temperatures that may be produced during high-intensity US sonications (~50°C) were performed. The mean values were obtained using four skulls, resulting in an observed shift in phase with temperature. Results, summarized in Fig 9, show the mean change in phase between room temperature measurements and elevated temperatures. A linear fit produces a slope of 0.29° of phase per °C.

DISCUSSION

This study examined major factors that may contribute to the phase of an US field at a specific point after propagating through a human skull. Each of the above models assumes that the skull thickness is approximately constant across that acoustic beam width. Additionally, the angle of incidence upon the skull was assumed to be normal and the inner and outer skull surfaces were assumed to be parallel. Although these assumptions create a simplification of the physical case, they allowed for rapid and straightforward calculations. It was not the goal of this study to provide a comprehensive model but, rather, to examine phase dependency on physical quantities that can readily be obtained using noninvasive imaging procedures, and to evaluate if the application of a given model could produce an improvement in a beam focused through a skull.

To evaluate a model, the study used two quantitative measurements of the error between the model and the experimental measurements. The first was the SD of all measured points. However, the use of SD alone is not a good indicator of the quality of a given model. Additional evaluation of the data are introduced in Fig. 5, which shows the percentage of points that deviate beyond a particular phase value.

Examination of the single-layer model indicates that phase shifts caused by the skull are clearly related to skull thickness, as shown in Fig. 4. However, a large SD (60°) from the homogeneous calculated value indicates additional sources must be considered. Possible error in the propagation speed does not account for this large deviation. A fit of the data using a least squares method gives a sound speed of 2.77×10^3 m/s and only improves the SD to 59°. At a frequency of 0.51 MHz, this sound speed is relatively close to the value of 2.65×10^3 m/s reported by Fry and Barger (1978), a 4.5% difference, and supports their result over published claims as high as 3.26×10^3 m/s (Hakim et al. 1997). A three-layer sound speed fit returned a trabecular bone speed equal to 2.45×10^3 m/s and a cortical speed of 3.15×10^3 m/s. It is noted that the calculated trabecular sound speed is significantly higher than measurements performed in weight-bearing cancellous bone (Laugier et al. 1997; Droin et al. 1998), where sound speed was found in the range of 1.5×10^3 m/s to 1.7×10^3 m/s.

The large error in the model indicates limitations on the use of a constant sound speed value and thickness to predict the phase shift caused by the skull bone, suggesting that other contributing factors need to be examined. Variation is introduced in the sound speed within internal skull layers and density is varied within the skull. The three-layer model divides the skull into a central layer surrounded by an inner and outer layer containing identical properties. It was determined that division into layers does not adequately improve results over the single-layer model. The SD of 60° recorded for the single layer becomes 59° for the three-layer model. Additional evaluation of the data examines the percentage of points that deviated beyond a particular phase value and also does not indicate improvement.

A density correction factor was taken from the average relative density through the skull. When applied to the single-layer model, a measurable improvement over the uncorrected case resulted in both the SD (56°), and particularly in the percent deviation (Fig. 7). Gradients of curves falling below this line indicate a larger number of data points with small phase error. When fit to an exponential function, $e^{-\alpha x}$, the constant in the exponent α provides a quantitative indicator of the quality of a model. The single-layer model was fit to an exponential function with a decay constant of $\alpha = 0.022$ and the

density-corrected case was fit to a value of $\alpha = 0.027$. When the curves were used as a probability distribution to add random error to the focal point of 1000 point sources, the thickness-corrected single-layer case expected a focal peak of 63% of the perfect value and the density-corrected case expected a focal peak of 76%. This is expected to allow adequate focusing for clinical transcranial US treatments.

Temperature-induced phase changes in the skull at 0.51 MHz were found to be less than 14° when the temperature was varied between 22°C and 50°C. This result implies that phase measurements performed at room temperature may be used for phase correction through a skull at body temperature. More importantly, the result suggests that temperature rises in the skull bone expected during a therapeutic treatment (~10°C) should not significantly change the phase.

Although temperature variation is not expected to cause major phase variation across the skull, other factors not presently considered can significantly affect the phase. These include the curvature of the skull, variation in density across the beam, and mode coupling. Although care was taken to align the transducer parallel with the skull surface, refraction at both the inner and outer skull surfaces was also not taken into account. Variation in thickness over the beam is not expected to contribute significantly to the overall error, based on the small variations in skull structure observed over the element size used. Internal reflection is also not expected to produce a major contribution to the overall phase, as studied in a previously reported experiment (Clement et al. 2001).

In conclusion, this study demonstrates that the phase correction prediction required for a US phased array to focus through a skull can be made, based on CT scan-derived bone thickness and density information. The measurements were performed using human skulls and, thus, the coefficients calculated from the results are directly applicable to clinical treatments.

Acknowledgements—This research was supported by grant CA76550 from the National Institutes of Health and by InSightec, Inc.

REFERENCES

Clement GT, Sun J, Giesecke T, Hynynen K. A hemisphere array for non-invasive ultrasound brain therapy and surgery. Phys Med Biol 2000a;45:3707–3719.

Clement GT, Sun J, Hynynen K. The role of internal reflection in transskull phase distortion. Ultrasonics 2001;39:109–113.

Clement GT, White JP, Hynynen K. Investigation of a large area phased array for focused ultrasound surgery through the skull. Phys Med Biol 2000b;45:1071–1083.

Droin P, Berger G, Laugier P. Velocity dispersion of acoustic waves in cancellous bone. IEEE Trans Ultrason Ferroelect Freq Control 1998;45:581–592.

Fry WJ. Production of focal destructive lesions in the central nervous system with ultrasound. J Neurosurg 1954;11:471–478.

Fry FJ, Barger JE. Acoustical properties of the human skull. J Acoust Soc Am 1978;63:1576–1590.

Fry FJ, Goss SA. Further studies of the transkull transmission of an intense focused ultrasonic beam: Lesion production at 500 kHz. Ultrasound Med Biol 1980;6:33–38.

Fry FJ, Goss SA, Patrick JT. Transkull focal lesions in cat brain produced by ultrasound. J Neurosurg 1981;54:659–663.

Hakim S, Watkin KL, Elahi MM, Lessard L. A new predictive ultrasound modality of cranial bone thickness. IEEE Ultrason Sympos 1997;2:1153–1156.

Hynynen K, Jolesz FA. Demonstration of potential noninvasive ultrasound brain therapy through an intact skull. Ultrasound Med Biol 1998;24:275–283.

Laugier P, Droin P, Laval-Jeantet AM, Berger G. In vitro assessment of the relationship between acoustic properties and bone mass density of the calcaneous by comparison of ultrasound parametric imaging and QCT. Bone 1997;20:157–165.

Robinson TC, Lele PP. An analysis of lesion development in the brain and in plastics by high-intensity focused ultrasound at low-megahertz frequencies. J Acoust Soc Am 1972;51:1333–1351.

Smith SW, Trahey GE, von Ramm OT. Phased array ultrasound imaging through planar tissue layers. Ultrasound Med Biol 1986;12:229–243.

Sun J, Hynynen K. Focusing of therapeutic ultrasound through a human skull: A numerical study. J Acoust Soc Am 1998;104:1705–1715.

Sun J, Hynynen K. The potential of transskull ultrasound therapy and surgery using the maximum available skull surface area. J Acoust Soc Am 1999;105:2519–2527.

Thomas J-L, Fink MA. UItrasonic beam focusing through tissue inhomogeneities with a time reversal mirror: Application to transskull therapy. IEEE Trans Ultrason Ferroelect Freq Control 1996;43:1122–1129.

Wear KA. Temperature dependence of ultrasonic attenuation in human cancaneus. Ultrasound Med Biol 2000;26:469–472.